Chemical Engineering Journal 148 (2009) 425–433

Contents lists available at ScienceDirect

Chemical Engineering Journal

journal homepage: www.elsevier.com/locate/cej

A novel study of hexavalent chromium detoxification by selected seaweed species using SEM-EDX and XPS analysis

Vanessa Murphy[a,*], Syed A.M. Tofail[b,1], Helen Hughes[a,2], Peter McLoughlin[a,3]

[a] Estuarine Research Group, Department of Chemical and Life Sciences, Waterford Institute of Technology, Cork Road, Waterford, Ireland
[b] Materials and Surface Science Institute, University of Limerick, Limerick, Ireland

ARTICLE INFO

Article history:
Received 14 May 2008
Received in revised form 2 September 2008
Accepted 17 September 2008

Keywords:
Biosorption
Seaweed
Hexavalent chromium
XPS
Reduction

ABSTRACT

The toxicity and mobility of Cr(VI) means that it is crucial that the amount of the heavy metal discharged in industrial waste streams is significantly decreased. Seaweed biomass represents a benign, cost-effective, sustainable and efficient solution for the detoxification of anionic Cr(VI) to the less hazardous cationic Cr(III). Chromium binding and reduction behaviour of three seaweeds, *Fucus vesiculosus* (brown), *Ulva* spp. (green) and *Palmaria palmata* (red), was investigated using a colorimetric method while the surface characteristics of the biomasses were examined using SEM/EDX and XPS techniques. This is the first study of red seaweeds for the detoxification of Cr(VI). Results indicated that *F. vesiculosus* and *P. palmata* had comparable total Cr removal efficiencies of approximately 18%, while *Ulva* spp. removed 14% Cr from a 2000 mg L^{-1} metal solution. Conversion of Cr(VI) to Cr(III) in solution ranged from 51% for *F. vesiculosus* to 34% for *Ulva* spp. over a 6-h period. SEM revealed considerable morphological differences between Cr(III) and Cr(VI)-loaded seaweeds while EDX results confirmed an ion-exchange mechanism for Cr(III) binding. XPS results indicated that significant quantities of Cr(VI) solution were reduced when placed in contact with the seaweed surface over a 6-h period, resulting in a 64–75% conversion to Cr(III) bound to the seaweed. Thus, the potential of these seaweeds to bio-reduce and detoxify elevated Cr(VI) concentrations over relatively short time periods has been demonstrated. Cr(VI) binding also altered the relative quantities of carboxyl and alcohol groups in biomass polysaccharides, thus indicating the importance of these functionalities in binding and reduction of Cr(VI) to Cr(III). This work, coupled with existing capacity data points towards the viability of these environmentally friendly biosorbents for use in packed columns in a number of industries including electroplating and tanning.

1. Introduction

The presence of heavy metals in industrial wastewater represents a serious environmental problem. The most important sources of chromium in the environment are from electroplating, tanning, water-cooling, pulp production as well as ore and petroleum refining processes [1]. While the effluents from these processes contain both Cr(VI) and Cr(III) ranging from tens to hundreds of mg L^{-1}, Cr(VI) is more hazardous to public health due to its greater mobility and mutagenic and carcinogenic properties. Thus the discharge of Cr(VI) into surface water is regulated to below 0.05 mg L^{-1} while total Cr, including Cr(III), Cr(VI), and its other forms, is regulated to below 2 mg L^{-1} [2]. Because of its toxicity, it is therefore increasingly important to identify methods for detoxification of Cr(VI) thus facilitating environmental cleanup.

Conventional chromium removal processes, including ion-exchange, activated carbon adsorption, reverse osmosis, and membrane filtration can be expensive or ineffective at low concentrations and may also lead to secondary environmental problems from waste disposal [3]. Thus, much research has been focussed on identifying biological materials that can efficiently remove heavy metals from aqueous environments. These materials are known as biosorbents and the passive binding of metals by living or dead biomass is referred to as biosorption [4].

Seaweeds are extremely efficient biosorbents with the ability to bind various metals from aqueous effluents [5,6]. Numerous chemical groups including carboxyl, sulphonate, hydroxyl and amino [7] may be responsible for metal biosorption by seaweeds. These functionalities act as binding sites for metals with their relative importance depending on factors such as the quantity of sites, their accessibility and the affinity between site and metal. The main metal binding mechanisms include physical adsorption,

* Corresponding author. Tel.: +353 51 306161.
E-mail addresses: vmurphy@wit.ie (V. Murphy), tofail.syed@ul.ie (S.A.M. Tofail), hhughes@wit.ie (H. Hughes), pmcloughlin@wit.ie (P. McLoughlin).
[1] Tel.: +353 61 213127.
[2] Tel.: +353 51 302064.
[3] Tel.: +353 51 302029.

1385-8947/$ – see front matter © 2008 Elsevier B.V. All rights reserved.
doi:10.1016/j.cej.2008.09.029

ion-exchange and complex formation [5] but these may differ according to biomass type, origin and the processing to which it has been subjected.

Biosorption processes are now becoming an extremely viable option due to the ready availability of non-living biomasses, lower operating costs and high efficiency metal removal. The current worldwide market for ion-exchange resins for heavy metal applications is in the order of 5 billion US dollars [8]. Biosorbents can be marketed for a fraction of ion-exchange costs thus making them extremely competitive products capable of opening whole new markets unavailable to high priced conventional technologies.

The present study investigates the potential of *Fucus vesiculosus* (brown), *Palmaria palmata* (red) and *Ulva* spp. (green) for Cr(VI) removal and detoxification in an industrial context. These seaweeds have not previously been studied for their Cr(VI) detoxification capacity thus illustrating the novelty of approach in this work. This study aims to quantify the removal and reduction of Cr(VI) from concentrated metal solutions as well as evaluating the characteristics of the biomaterial during chromium biosorption. Characterisation is achieved using Scanning Electron Microscopy/Energy dispersive X-ray analysis (SEM/EDX) and X-ray photoelectron spectroscopy (XPS) which identifies key functionalities responsible for metal binding and allows the elucidation of chromium binding mechanisms to these seaweeds.

2. Materials and methods

2.1. Preparation of the biomass

The brown seaweed *F. vesiculosus*, the green seaweed *Ulva* spp. and the red seaweed *P. palmata* were harvested from Fethard-on-Sea, Co. Wexford, Ireland (52°11′53.68″N, 64°9′34.36″W). The samples were rinsed thoroughly with distilled water in order to remove any adhering debris, cut into pieces between 3 and 5 mm, then subsequently oven-dried at 60 °C for 24 h. Samples were stored in air-tight containers until required.

2.2. Cr(VI) biosorption experiments

Cr(III) and Cr(VI) solutions (2000 mg L^{-1}) were freshly prepared using analytical grade $Cr(NO_3)_3{\cdot}9H_2O$ and $K_2Cr_2O_7$ (Sigma–Aldrich) dissolved in distilled water. For the binding studies, 100 mg of biomass was exposed to 50 mL of Cr solution. Flasks were shaken for 6 h at 200 rpm and room temperature (21 ± 1 °C) with the solution pH maintained at optimum values using 0.1 M HCl and NaOH. Earlier sorption experiments by Murphy et al. [9] revealed that these values were pH 4.5 and 2 for Cr(III) and Cr(VI), respectively. Following exposure, the biomass was filtered under vacuum, washed with distilled water and oven dried at 60 °C for 24 h. The filtrate was stored in acid-washed plastic bottles at 4 °C before analysis. After appropriate dilution of samples, total chromium (i.e. Cr(III) and Cr(VI)) in the filtrate was measured by Inductively Coupled Plasma Optical Emission Spectroscopy (ICP-OES) (Varian 710-ES). The Cr(VI) concentration of the filtrates was subsequently determined using a colorimetric method [10]. Samples were analysed by UV at 540 nm after complexation with 1,5-diphenylcarbazide and the Cr(III) concentration was then obtained by difference. All experiments were performed in triplicate.

2.3. Scanning Electron Microscopy with combined energy dispersive X-ray analysis

Dehydrated raw and Cr-loaded samples were attached to 10 mm metal mounts using carbon tape and sputter coated with gold under vacuum in an argon atmosphere. The surface morphology of the coated samples was visualized by a Scanning Electron Microscope (Hitachi S4000) with combined Energy Dispersive X-ray Analyser at a voltage of ~10 keV. SEM allowed the identification of any interesting structural features on the seaweed surface with EDX used to determine the elemental composition of the surface before and after Cr binding.

2.4. X-ray photoelectron spectroscopy analysis

Raw and Cr-loaded samples were mounted on insulating double-sided tape attached to a stainless steel holder and loaded in a sample treatment chamber, which was then pumped down to a pressure of 10^{-6} Pa. The sample holder was then transferred to the analysis chamber of a Kratos Axis 165 X-ray Photoelectron Spectrometer, the pressure of which was always better than 10^{-7} Pa. Three points on each sample were randomly selected and focussed for optimum photoelectron intensity. Low resolution survey spectra were acquired in the binding energy range of 1400 and −2 eV at 160 eV pass energy while high resolution narrow range spectra for elements of interest were acquired at 20 eV pass energy. A monochromatic Al Kα (excitation energy 1486.6 eV) at a voltage of 10 kV and a current of 15 mA was used. The surface charge on the seaweed samples was neutralised by a coaxial charge neutraliser. The acquired spectra were corrected using the C 1s position for C–C bonding at 285 eV as reference. The thickness of the analysed layer was 50–100 Å. The compounds $CrCl_3{\cdot}6H_2O$ and $K_2Cr_2O_7$ (Sigma–Aldrich) were used as Cr(III) and Cr(VI) references, respectively.

3. Results and discussion

3.1. Reduction of Cr(VI) to Cr(III)

Seaweed functionalities such as sulphonate ($-OSO_3$) and carboxyl (–COOH) display acidic characteristics and therefore, the pH at which maximum metal uptake occurs is related to the pK_a of these groups. The point of zero charge (PZC) of these seaweeds was previously determined by Murphy et al. [11] and on average, a value of approximately of 6.18 was observed. Thus, below the PZC the biomass still has a net positive charge despite the presence of dissociated negatively charged functionalities. As a result, pH variation will significantly affect the binding behaviour of chromium species. Murphy et al. [9] identified that the optimum pH for Cr(III) sorption was 4.5 while that for Cr(VI) was pH 2. At pH values <3, competition from H^+ ions for biomass binding sites contributes to decreased Cr(III) binding. However, as pH increases, fewer H^+ ions are present in solution thus resulting in less competition for binding sites and hence increasing Cr(III) uptake.

The pH range dependence of Cr(III) uptake suggests that carboxyl groups (pK_a 3.5–5.0) are important in binding. Murphy et al. [9] identified various carboxyl functionalities with pK_a values in this range for the seaweeds under investigation. The quantities of these groups were 2.00 mmol g^{-1} for *F. vesiculosus*, 1.5 mmol g^{-1} for *Ulva* spp. and 1.12 mmol g^{-1} for *P. palmata*. Therefore, it was expected that carboxyl groups would significantly influence metal binding in these seaweeds.

Sheng et al. [13] also showed that sulphonate groups (pK_a 1.0–2.5) may also contribute to metal binding at low pH. The interaction of –COOH and $-OSO_3$ functionalities with Cr(III) was shown by decreased, but not negligible, metal uptake at low pH. At pH > 3.5, dissociation of these functionalities leads to increased negative charge on the biomass, so, while anionic Cr(VI) species are repelled at these pHs, cationic Cr(III) experiences increased

Table 1
Chromium removal and reduction from a concentrated metal solution. Initial Cr(VI) concentration = 2000 mg L^{-1}, biomass concentration = 2 mg mL^{-1}, Exposure time = 6-h, pH 2. Error bars are ±1 standard deviation based on triplicate samples.

Seaweed	Total Cr remaining in solution (mg L^{-1})	Removal efficiency (%)	Cr(VI) (mg L^{-1})	Cr(III) (mg L^{-1})	Cr(VI) q_{max} (mmol g^{-1})[a]	Cr(VI) b (L $mmol^{-1}$)[a]
F. vesiculosus	1627 ± 19	18.65 ± 0.15	795 ± 12	831 ± 30	0.82 ± 0.04	1.76 ± 0.16
Ulva spp.	1707 ± 25	14.65 ± 0.35	1117 ± 41	590 ± 66	0.58 ± 0.07	1.20 ± 0.12
P. palmata	1633 ± 32	18.35 ± 0.20	930 ± 22	702 ± 55	0.65 ± 0.09	8.64 ± 0.31

[a] Chromium binding data obtained from Murphy et al. [11].

attraction to the biomass resulting in improved metal binding. As solution pH decreases, functionalities such as amino (–NH_2) and carboxyl groups may become protonated, thus making the biomass more positively charged and hence creating an electrostatic attraction with Cr(VI) species.

From Table 1 it is seen that, at an initial Cr(VI) concentration of 2000 mg L^{-1}, *F. vesiculosus* and *P. palmata* were comparable in terms of their overall Cr removal efficiency (18.65 and 18.35%, respectively), with *U.* spp. having a slightly lower efficiency of 14.65%. This trend is in agreement with previous isotherm studies for Cr(VI) which revealed that the maximum capacities of these seaweeds decreased in the order *F. vesiculosus* > *P. palmata* > *U.* spp. [9] (Table 1). *Ulva* spp. also had the lowest affinity for Cr(VI) as predicted by Langmuir *b* values (1.20 L $mmol^{-1}$).These results are also well aligned with those of Park et al. [28] who reported that the removal efficiencies of *Ecklonia* biomass, at initial Cr(VI) concentrations of 1000 and 5000 mg L^{-1} were 66.4 and 26.2%, respectively after 10 days. Therefore, the concentration removed in a 6 h period in this study was larger than previously seen in the literature and results show improved efficiency for these seaweeds.

In order to ascertain the relative quantities of Cr(VI) and Cr(III) remaining in solution, a colorimetric method using 1,5-diphenylcarbazide was employed. Results indicated that, in solution *F. vesiculosus* displayed the greatest concentration of Cr(III) (51%) followed closely by *P. palmata* (43%). *U.* spp. had a much lower conversion to Cr(III) in solution having only 34% of the species. The presence of Cr(III) in solution may result from either direct conversion of Cr(VI) in the aqueous phase or alternatively from an indirect method of Cr(VI) binding by the biomass, reduction to Cr(III) and release back into solution due to electronic repulsion.

While *Ulva* spp. appeared to be the weakest performer in terms of overall removal efficiency and solution conversion of Cr(VI) to Cr(III), subsequent XPS results will show its superior capacity for Cr(VI) detoxification on the biomass surface.

From a practical viewpoint, significant Cr(VI) removal over a shorter time period would prove especially important in an industrial context, whereby increased contact times lead to increased process costs.

3.2. Scanning Electron Microscopy/energy dispersive X-ray analysis

3.2.1. SEM analysis

SEM micrographs (Fig. 1) revealed considerable differences in surface morphology between the brown, green and red seaweeds. This potentially results from compositional differences in terms of cell wall polysaccharides and proteins [12].

All three seaweed types contain cellulose in their inner cell wall with the outer cell wall consisting of an amorphous embedding matrix [5]. In brown seaweeds this matrix is predominately alginic acid with small amounts of sulphated fucoidan, in reds it is made up of xylans and several sulphated galactans including agar and carrageenan while in the greens, it consists of both xylans and mannans [12]. This variation in polymer type results in different quantities of available functionalities on the seaweeds, e.g. –COOH, –NH_2, –OSO_3, and –OH. Variation in the quantity of acidic binding sites was reported by Murphy et al. [9] where *F. vesiculosus* had the greatest number (2.44 mmol g^{-1}), followed by *Ulva* spp. (1.94 mmol g^{-1}) and *P. palmata* (1.31 mmol g^{-1}). The quantity and availability of these groups will thus have a major influence on

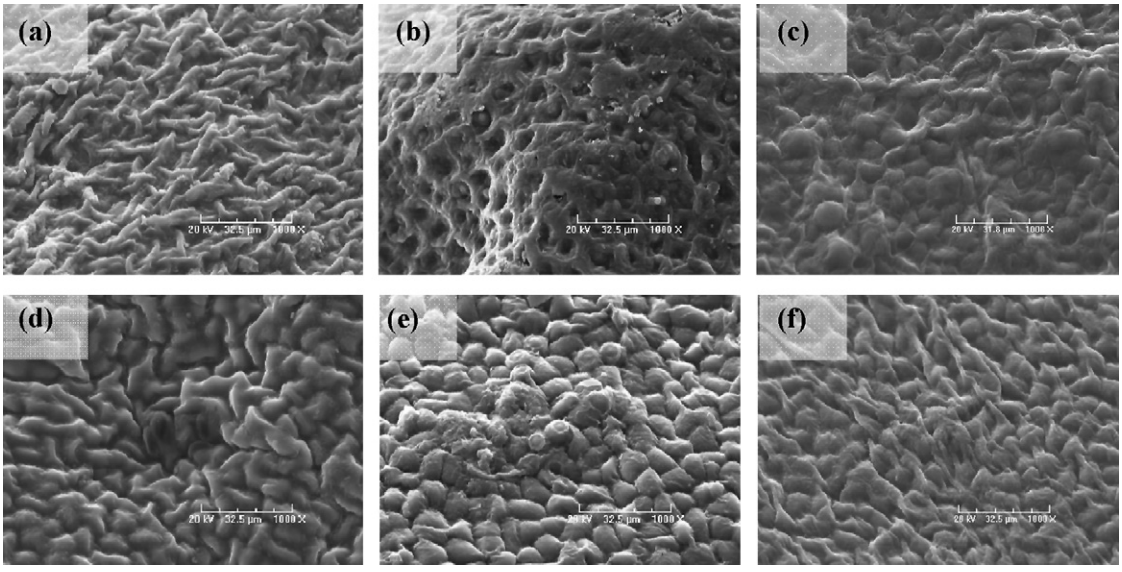

Fig. 1. SEM micrographs of raw and Cr-loaded seaweeds at a magnification of 1000× where (a), (b) and (c) represent: raw, Cr(III)-loaded and Cr(VI)-loaded *Ulva* spp. and (d), (e) and (f) are: raw, Cr(III)-loaded and Cr(VI)-loaded *P. palmata*.

chromium binding to the seaweed surface indicating that metal binding is related to seaweed composition.

A number of authors have previously used SEM to identify morphological changes in seaweeds with particular focus on the brown seaweed *Sargassum* sp. [14,15]. Chen et al. [16] have also used the technique to study the morphology of an alginate-based resin before and after Cu(II) binding.

In the current study, the effect of Cr(III) on surface morphology has been included to facilitate comparison between cationic Cr(III) and anionic Cr(VI)-binding behaviour. When raw seaweeds are exposed to Cr(III) solutions, metal cations may replace some of the alkali and alkaline earth metals naturally present in the cell wall, i.e. K(I), Na(I), Ca(II), and Mg(II). Raize et al. [14] proposed that replacement of these ions with metal cations altered the nature of the cross-linking due to stronger electrostatic and coordinative bonding between the metal and negatively charged groups in the cell wall polymers. Thus, changes in surface morphology should be readily apparent. The surface morphology of *Ulva* spp. and *P. palmata* before and after chromium binding is illustrated in Fig. 1

After Cr binding, the surface of *F. vesiculosus* (not shown) appears flattened in comparison to the raw sample. In the Cr(III)-laden sample the formation of repeating row structures was apparent but no significant morphological changes were discernable after Cr(VI) binding. In Fig. 1, considerable changes were apparent in *Ulva* spp. after Cr binding. Raw *Ulva* spp. has fold-like structures in a random arrangement on the surface (Fig. 1a) but these are not present in the Cr(III)-loaded images (Fig. 1b). The Cr(VI)-loaded surface displayed large morphological changes with the formation of mound-like structures and an apparent flattening of the seaweed surface (Fig. 1c). The Cr(VI)-loaded surface resembles raw seaweed morphology more closely than Cr(III)-loaded samples, thus illustrating potential differences in Cr(III) and Cr(VI)-binding mechanisms as seen in adsorption studies.

The results obtained in this study are in agreement with the work of Chen et al. [16] who observed changes in surface morphology of a Ca-alginate-based resin after Ca(II) ions were replaced with Cu(II) ions. Similarly to Cu(II) ions (ionic radius: 0.71 Å), Cr(III) offers a smaller coordination sphere and ionic radius than Ca(II) (0.63 Å for Cr(III) versus 1.14 Å for Ca(II)). Therefore, the coordination sphere of Cr(III) incorporates a smaller number of hydroxyl and carboxyl groups than that of Ca(II) [16]. Thus, surface polymer chains are less twisted in the Cr(III) bound matrix, hence the apparently flattened surface. Yang and Chen [15] also reported that, for Cr(VI) binding to *Sargassum* sp., changes in surface morphology were due to an exchange of the desired metal with alkali metals causing relaxation of the biomass structures thus leading to an apparent flattening of the seaweed surface.

With an ionic radius of 0.58 Å, Cr(VI) binding to these seaweeds should theoretically result in a flattened structure if some ion-exchange takes place. However, from Fig. 1c and 1f, it is clear that the folded structures originally present in the raw seaweed are still visible to a certain extent in the Cr(VI)-loaded seaweed. This indicates that some changes in surface structure have taken place after Cr(VI) binding but in a different manner to Cr(III) binding.

Raw *P. palmata* (Fig. 1d) contains fold structures similar to those observed in *Ulva* spp. but in the former these structures are fewer and less pronounced giving the surface a rougher appearance. Mound-like structures on the surface of Cr(III)-loaded *P. palmata* (Fig. 1e) indicates some rearrangement of surface polymer chains while the Cr(VI)-loaded sample (Fig. 1f) reveals differences in surface morphology which are quite distinct from Cr(III)-loaded samples. Again this points to differences between cation and anion binding which require further investigation.

3.2.2. EDX analysis

Figueira et al. [17] and Kuyucak and Volesky [18] observed a decrease in the concentration of alkali and alkaline earth metals after metal exposure in *U. lactuca* and *A. nodosum* indicating that ion-exchange is significant for cation binding to seaweeds. The significant EDX peaks observed in this study for raw and Cr-loaded *F. vesiculosus* are shown in Fig. 2. Similar results were obtained for *U.* spp and *P. palmata*.

The absence of alkali and alkaline earth metal peaks (Na^+, K^+, Ca^{2+} and Mg^{2+}) in the Cr(III)-loaded seaweeds (Fig. 2b) in this study indicates the existence of a significant ion-exchange mechanism for cation binding. However, the Cr(VI)-loaded samples (Fig. 2c) revealed no discernable changes in elemental composition, apart from the presence of chromium, indicating that ion-exchange was not the dominant mechanism of Cr(VI) binding to these species. Therefore, the binding of Cr(VI) to these seaweeds was further investigated using XPS analysis.

As this technique has been used only qualitatively and the scale used for the EDX spectra is arbitrary, unless a peak is absent after metal binding, it is difficult to evaluate changes in peak size or intensity. Therefore, even though previous FTIR analyses [9] indicate significant involvement of sulphur and oxygen containing functionalities for both Cr(III) and Cr(VI) biosorption, it was not possible to evaluate metal interactions with these elements using non-quantitative EDX.

3.3. Cr(VI)-binding studies using XPS

In order to characterise the main Cr(VI) removal mechanisms, it is important to determine the oxidation state in which the chromium is bound [19]. For example, if only Cr(III) is present, it can be concluded that Cr(VI) is completely reduced to Cr(III) by the biomass. Previous studies have investigated the species of chromium bound in various types of dead biomass. Lytle et al. [20] reported that Cr(VI) taken from the fine lateral roots of wetland plants was rapidly reduced to Cr(III) while Gardea-Torresdey et al. [21] reported that Cr(VI) could be bound to an oat by-product, but was easily reduced to Cr(III) by positively charged functional groups, and subsequently bound to carboxyl groups.

While the EDX results in Section 3.2.2 offer a qualitative estimation of the elemental changes after Cr(III) binding, no such information is provided for Cr(VI) binding. XPS offers a more quantitative picture of these changes after Cr(VI) binding and acts as a support for the results previously obtained by FTIR analysis [9]. It also identifies the functionalities involved in binding as well as facilitating elucidation of Cr binding mechanisms to these seaweeds.

3.3.1. Survey spectra

The elemental composition of the raw and Cr(VI)-loaded seaweeds as found in survey spectra are summarised in Table 2 with only the elements of interest in binding shown.

From Table 2, it is clearly seen that the seaweeds had relatively large amounts of Cr associated with their surface after exposure. Results indicated that *F. vesiculosus* and *P. palmata* had comparable amounts of chromium bound to their surfaces (1.13 and 1.14%, respectively) while a lower quantity was bound to *Ulva* spp. (0.76%). These results agree with earlier sorption isotherm results [9] which showed that *F. vesiculosus* and *P. palmata* had similar q_{max} values (0.68 and 0.65 mmol g^{-1}, respectively) for Cr(VI) sorption while *Ulva* spp. had a q_{max} value of 0.58 mmol g^{-1}.

No appreciable changes were found in the atomic concentration of carbon for *F. vesiculosus* and *P. palmata* (Table 2) but a decrease in the carbon content of *Ulva* spp. from 62 to 55% was noted after Cr-loading thus indicating some biomass leaching dur-

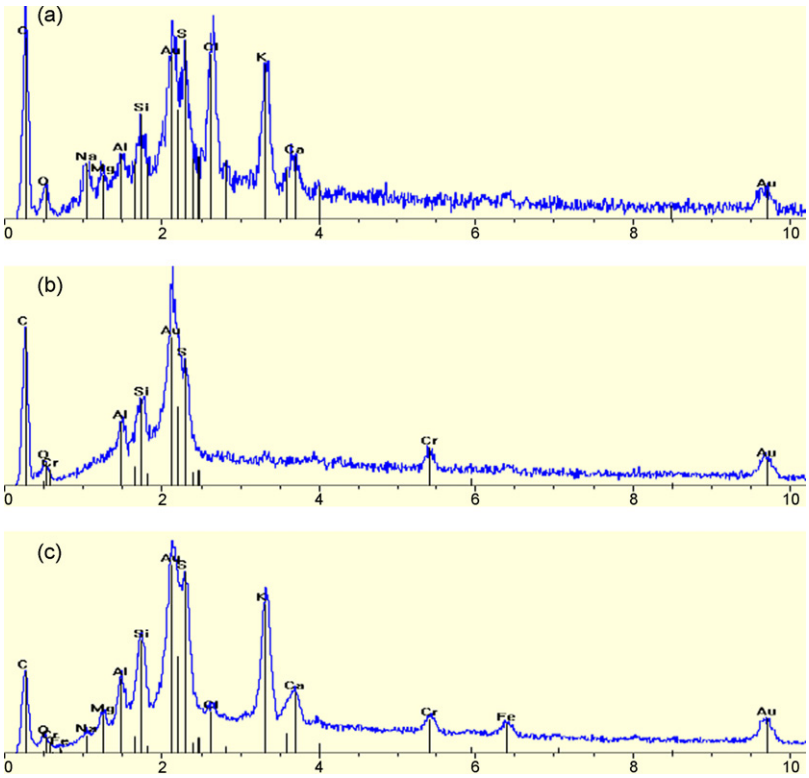

Fig. 2. EDX spectra of (a) raw, (b) Cr(III), and (c) Cr(VI)-loaded *Fucus vesiculosus*. Magnification: 1000×. Au peak is associated with gold sputter coating; Al originates from sample holder and Fe peak may be due to surface contamination.

ing the experiment [16]. While there was no appreciable change in the O concentration of *F. vesiculosus* after Cr(VI) binding, both *Ulva* spp. and *P. palmata* showed an increase in O concentration from approximately 24 to 29%. This increased concentration may potentially be due to the adsorption of chromium hydroxides during the metal-binding process.

Nitrogen levels in *Ulva* spp. (8.01%) were almost double that in *P. palmata* (4.66%) or *F. vesiculosus* (4.13%) which may indicate a higher proportion of surface proteins in *Ulva* spp. Wong and Cheung [22] found that *Ulva lactuca* had high concentrations of glutamic acid, aspartic acid and alanine among other amino acids which contributes to increased quantities of N. While previous FTIR analysis [9] illustrated the importance of amino functionalities in Cr(VI) binding, no significant change in N levels was found for these seaweeds after Cr binding.

No significant changes in overall S concentration were observed after Cr(VI) exposure but their importance in Cr(VI) binding was previously illustrated in FTIR studies [9] and potentiometric titration [9].

Both Raize et al. [14] and Yang and Chen [15] found that, for *Sargassum* sp., higher levels of oxygen (38.40–42.03%) were present than in the three seaweeds in the present study (Table 2) which may be due to increased quantities of carboxyl functionalities in this species [9]. A lower carbon atomic concentration (47.44–47.60%) was also observed by these authors [14,15] but sulphur (0.65–1.14%) and nitrogen (3.52–6.91%) levels were comparable for all studies.

3.3.2. Narrow range spectra

The narrow range C1s spectra in Fig. 3 depict multiple oxidation states of carbon with peaks summarised in Table 3. The spectra are comprised of four main peaks with the arbitrary units on the *y*-axis describing the number of electrons arriving on the detector per unit time [23].

The peak with a binding energy (BE) of 285 eV is attributed to C–C/C–H bonding and these hydrocarbon functionalities are used for energy calibration of the instrument [24]. The remaining peaks can be assigned to alcoholic (C–O), ether (O–C–O) and carboxyl (O=C–O) groups with BE of 286, 288 and 289 eV, respectively [16]. These organic functionalities are typical in algal polysaccharides and variation in BE occurs because the carbon atoms in these groups possess different electron densities [25]. The additional presence of N and S will cause chemical shifts of these peaks to higher binding energies, whereas C bonded to metals such as Cr will cause a chemical shift towards the lower binding energy side such as those observed in Table 3.

Table 2
Elemental composition of raw and Cr(VI)-loaded seaweeds as determined using XPS. Average data from triplicate analyses are given with ±1 standard deviation quoted.

Elements	Average atomic concentration (%)					
	F. vesiculosus	*U.* spp.	*P. palmata*	Cr-loaded *F. vesiculosus*	Cr-loaded *U.* spp.	Cr-loaded *P. palmata*
C 1s	67.21 ± 0.77	62.41 ± 1.99	68.98 ± 5.24	65.33 ± 3.76	55.31 ± 7.03	63.71 ± 1.43
N 1s	4.13 ± 0.49	8.01 ± 0.45	4.66 ± 0.43	3.32 ± 0.46	6.74 ± 1.44	4.59 ± 1.33
O 1s	27.77 ± 0.54	24.01 ± 2.40	24.54 ± 3.09	28.44 ± 2.34	29.77 ± 6.30	29.22 ± 2.48
S 2p	0.73 ± 0.11	1.03 ± 0.45	0.56 ± 0.08	0.57 ± 0.21	0.79 ± 0.32	0.61 ± 0.09
Cr 2p	–	–	–	1.13 ± 0.21	0.76 ± 0.19	1.14 ± 0.11

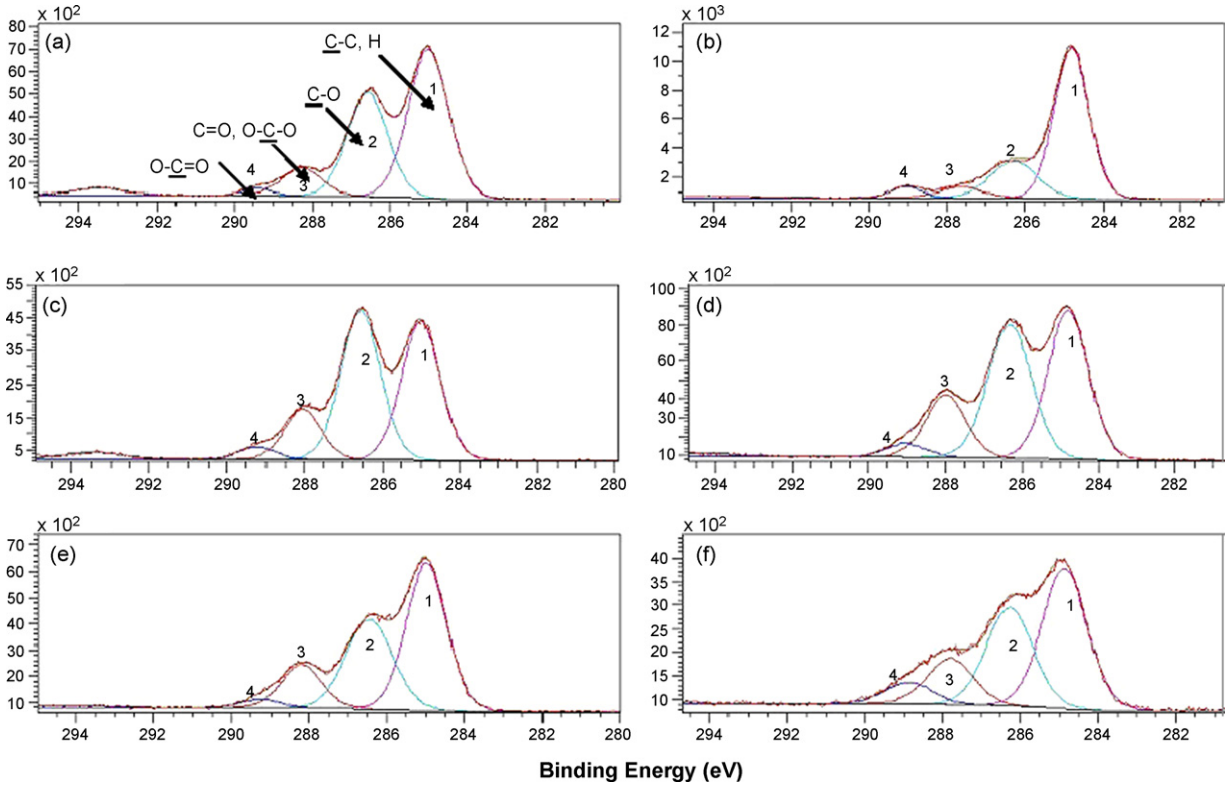

Fig. 3. C1s photoelectron spectra for *F. vesiculosus* (a) raw, (b) Cr-loaded; *P. palmata*, (c) raw and (d) Cr-loaded; *Ulva* spp. (e) raw and (f) Cr-loaded. Initial Cr(VI) concentration = 2000 mg L^{-1}, biomass concentration = 2 mg mL^{-1}, exposure time = 6 h, pH 2.

From Table 3, it is seen that the C–C content in Cr-loaded *Ulva* spp. (37%) and *P. palmata* (45%) does not vary from that in the raw seaweed (within error) indicating that there was limited organic leaching during metal exposure. On the other hand, the C–C content of *F. vesiculosus* increased considerably from 51 to 61% after Cr-loading, thus pointing to potential surface contamination during exposure [16]. The raw C1s spectrum of *P. palmata* (Fig. 3c) is dominated by high proportion of C–O bonding (Peak 2). Apart from *F. vesiculosus* which decreases from 33 to 22%, the C–O proportion is virtually unchanged by the addition of Cr. The relative proportion of O–C–O (Peak 3) bonding also shows little sensitivity due to Cr-loading in all cases. However, for all seaweeds, the proportion of carboxylate groups (Peak 4) increases after Cr binding. This is in agreement with the findings of Yang and Chen [15] who reported that Cr(VI) anions could oxidise secondary alcohol groups on biosorbents, while undergoing reduction to Cr(III). Results also correlate with the observed decrease in the proportion of C–O functionalities as discussed and are in agreement with previous FTIR studies which showed carboxyl group interactions to be one of the most important in chromium binding to these seaweeds [9].

A high proportion of O in these samples was clearly expected given the large amounts of cell wall polysaccharides present on the seaweed surface (Table 2). Unresolved spectra of raw and Cr-loaded (not shown) revealed that the O 1s band was shifted to a lower BE in all cases after Cr(VI) exposure: 533–532.4 eV (*F. vesiculosus*), 533–532.6 eV (*P. palmata*) and 532.4–532 eV (*Ulva* spp.). This finding, coupled with additional binding data (Table 3) suggests chemical adsorption of chromium on the surface. Narrow

Table 3
Components of raw and Cr(VI)-loaded seaweed XPS C 1s spectra and their relative distribution. Average data from triplicate analyses are shown. Error bars are ±1 standard deviation.

Sample	Component	Energy position ±S.D. (eV)	Relative amount ±S.D. (%)	Sample	Energy position ±S.D. (eV)	Relative amount ±S.D. (%)
F. vesiculosus						
Raw	C–C/C–H	285.00 ± 0.01	51.11 ± 1.03	Cr-loaded	284.86 ± 0.12	61.34 ± 3.67
	C–O	286.55 ± 0.01	33.88 ± 1.27		286.40 ± 0.15	22.31 ± 2.71
	C=O, O–C–O	288.22 ± 0.07	7.74 ± 0.94		287.80 ± 0.22	6.81 ± 0.63
	COO	289.21 ± 0.19	2.99 ± 0.76		289.14 ± 0.12	4.78 ± 0.23
P. palmata						
Raw	C–C/C–H	285.00 ± 0.00	37.13 ± 1.65	Cr-loaded	284.79 ± 0.01	37.68 ± 4.71
	C–O	286.53 ± 0.02	43.22 ± 0.95		286.33 ± 0.03	40.87 ± 4.33
	C=O, O–C–O	288.03 ± 0.02	12.45 ± 1.07		287.95 ± 0.08	13.89 ± 1.05
	COO	289.14 ± 0.11	3.66 ± 0.18		288.89 ± 0.19	4.45 ± 1.13
U. spp.						
Raw	C–C/C–H	284.99 ± 0.01	46.22 ± 1.48	Cr-loaded	284.83 ± 0.03	45.01 ± 3.21
	C–O	286.46 ± 0.02	33.04 ± 0.33		286.24 ± 0.02	32.21 ± 3.57
	C=O, O–C–O	288.17 ± 0.04	13.11 ± 1.01		287.81 ± 0.07	14.67 ± 2.55
	COO	289.13 ± 0.17	3.91 ± 0.76		288.97 ± 0.09	6.22 ± 0.43

Table 4
Components of raw and Cr(VI)-loaded seaweed XPS O 1s spectra and their relative distribution. Average data from triplicate analyses are shown. Error bars are ±1 standard deviation.

	Identification	*F. vesiculosus*				*P. palmata*				*Ulva* spp.			
		BE position (eV)		Relative proportion (%)		BE position (eV)		Relative proportion (%)		BE position (eV)		Relative proportion (%)	
		Raw	Cr-loaded	Raw	Cr-loaded	Raw	Cr-loaded	Raw	Cr-loaded	Raw	Cr-loaded	Raw	Cr-loaded
1	M–O, e.g. Cr_2O_3/CrO_3	530.87	530.9	4.33	5.28	530.88	530.97	2.90	7.51	530.84	530.95	5.56	9.91
2	M–OH, e.g. $Cr(OH)_3$	531.66	531.77	18.09	22.79	531.64	531.57	15.44	23.54	531.65	531.68	33.93	28.77
3	C=O, $–SO_3$, SiO_2	532.49	532.41	28.99	39.88	532.55	532.45	22.73	38.55	532.52	532.41	28.01	34.21
4	C–O	533.25	533.17	34.77	21.23	533.19	533.10	49.77	25.81	533.34	533.16	24.98	18.22
5	C–O in COO group	533.96	533.91	12.01	9.56	534.14	534.02	6.35	3.27	534.09	534.39	6.41	7.75

range O 1s spectra are comprised of five components spanning the region 529–535.5 eV. An assignment of these peaks is given in Table 4.

As expected, there is a general increase in component 1 after Cr(VI) exposure which can be assigned to the existence of chromium oxide on the seaweed surface. The relative increases in this component are: 0.89% for *F. vesiculosus*, 4.47% for *P. palmata* and 4.67% for *Ulva* spp. While there is an increase in the relative proportion of component 2 (Cr hydroxides) for *F. vesiculosus* (4.70%) and *P. palmata* (7.89%) after Cr-loading, there is a decrease of 5.26% for *U.* spp. that is reflected in the reduced quantities of Cr bound by this seaweed.

Results showed that there was a general tendency for component 3 (C=O) to increase significantly after Cr loading. Increases of 11.53, 14.70 and 6.44% were observed for *F. vesiculosus*, *P. palmata* and *U.* spp., respectively. From Table 4, it is clearly seen that component 5 (C–O in –COO) decreased significantly after Cr(VI) loading and this, coupled with a corresponding increase in the relative amounts of carboxyl functionalities in the C 1s spectra (Table 3) potentially indicates a chemical adsorption with oxidation of C–O due to Cr loading.

Narrow range spectra (not shown) revealed the presence of protonated N in the form of –NH or $–NH_2$. The importance of these groups in metal binding has previously been demonstrated by FTIR [9] and chemical modification where blocking of these groups ($–NH_2$) resulted in decreased metal binding. According to Table 2, the seaweeds contained relatively small amounts of S with narrow range spectra indicating the presence of oxygenated sulphur in the form of sulphonate groups. Again, this is in agreement with earlier FTIR results [9] which confirm the presence of sulphonate groups on the seaweed surface and titrimetric work [9] showing that *Ulva* spp. had the largest quantity sulphonate functionalities (0.44 mmol g^{-1}) contributing to metal binding.

3.3.3. Chromium

Dambies et al. [26] reported that the Cr $2p_{3/2}$ orbitals are assigned at 577.2 eV ($CrCl_3$) and 576.2–576.5 eV (Cr_2O_3) for Cr(III) compounds, while Cr(VI) forms are characterised by higher binding energies such as 578.1 eV (CrO_3) or 579.2 eV ($K_2Cr_2O_7$). Therefore, by comparing the Cr peaks observed, it is possible to establish whether the bound Cr is in trivalent or hexavalent form and also identify the proportion of each oxidation state. The Cr 2p spectra

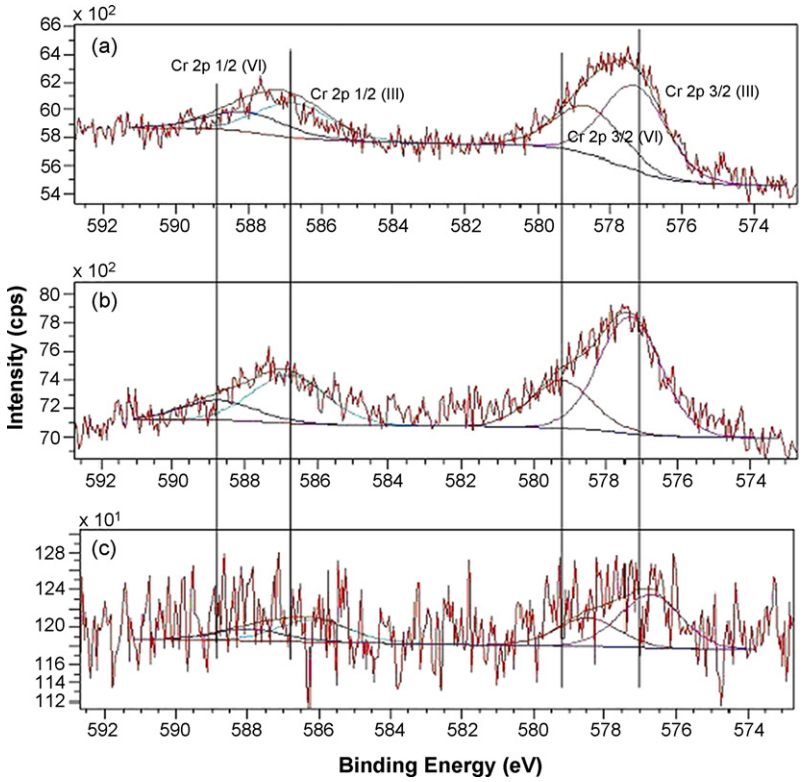

Fig. 4. Cr 2p spectra of Cr-loaded seaweeds (a) *F. vesiculosus*, (b) *P. palmata*, (c) *Ulva* spp. Initial Cr(VI) concentration = 2000 mg L^{-1}, biomass concentration = 2 mg mL^{-1}, exposure time = 6 h, pH 2.

Table 5
Components of Cr 2p high-resolution spectra for Cr(VI)-loaded seaweed samples as obtained using XPS. Initial Cr(VI) concentration = 2000 mg L^{-1}, biomass concentration = 2 mg mL^{-1}, exposure time = 6 h, pH 2.

Sample	Peak	Position (eV)	Relative proportion (%)	Cr(III)/Cr(VI) ratio
F. vesiculosus	Cr $2p_{3/2}$ (III)	577.53	64.21	1.79
	Cr $2p_{1/2}$ (III)	586.98		
	Cr $2p_{3/2}$ (VI)	579.43	35.79	
	Cr $2p_{1/2}$ (VI)	588.93		
Ulva spp.	Cr $2p_{3/2}$ (III)	577.52	74.79	2.97
	Cr $2p_{1/2}$ (III)	586.97		
	Cr $2p_{3/2}$ (VI)	580.18	25.22	
	Cr $2p_{1/2}$ (VI)	589.68		
P. palmata	Cr $2p_{3/2}$ (III)	577.21	68.96	2.22
	Cr $2p_{1/2}$ (III)	586.66		
	Cr $2p_{3/2}$ (VI)	579.27	31.04	
	Cr $2p_{1/2}$ (VI)	588.77		

of the seaweeds in the present study are illustrated in Fig. 4 with Cr-binding data summarised in Table 5.

Various studies have shown the effectiveness of the brown seaweed *Ecklonia* in reducing toxic Cr(VI) to the less toxic Cr(III) [29,30]. Cr(VI) reduction can be either direct (A) or indirect (B). In mechanism A, Cr(VI) is directly reduced to Cr(III) in the aqueous phase by contact with electron-donor groups on the biomass. Reduced Cr(III) either remains in the aqueous phase or may form complexes with biomass Cr-binding groups. Mechanism B, however, consists of three steps: (1) the binding of anionic Cr(VI) to positively charged groups on the biomass surface, (2) the reduction of Cr(VI) to Cr(III) by adjacent electron-donor groups, and (3) the release of the reduced Cr(III) into the aqueous phase due to electronic repulsion between positively charged groups and Cr(III), or the complexation of the reduced Cr(III) with adjacent groups, i.e., Cr-binding groups. Carboxyl and amino groups have been shown to be especially important in Mechanism B and this is in agreement with titrimetric and FTIR results shown by Murphy et al. [9] for the binding of Cr(VI) to seaweed biomass.

While the biomasses were exposed only to Cr(VI) solutions, there is evidence of both Cr(III) and Cr(VI) on the biomass surface (Fig. 4). This indicates that both Cr(VI) adsorption and reduction are involved in binding to these seaweeds (Mechanism B). An estimation of the Cr(III)/Cr(VI) ratio reveals that, in the case of *P. palmata* and *Ulva* spp., the proportion of Cr(III) on the seaweed surface is more than double that of Cr(VI) (2.22 and 2.97, respectively), while for *F. vesiculosus*, this value is slightly less than double (1.79). Both the biomass and metal concentrations (2 mg mL^{-1} and 2000 mg L^{-1}, respectively) were kept constant for all three seaweeds, thus implying that, of the seaweeds studied, *Ulva* spp. had the greatest Cr(VI) reduction capacity. The presence of reduced Cr in all seaweeds indicates that it is not simply brown seaweeds that possess the ability to reduce significantly large concentrations of Cr(VI).

Park et al. [27] also studied Cr(VI) reduction by the green seaweed *Enteromorpha* as part of a wider study of 16 biomaterials but to date, no work on the reduction of Cr(VI) by red seaweeds has been found in the literature. In their study of Cr (VI) biosorption onto *Sargassum* sp., Yang and Chen [15] showed that the raw seaweed reduced 48% of the Cr(VI) to Cr(III) at pH 1 and 77% of Cr(VI) at pH 2 (initial concentration = 1 mM) and a contact period of 24 h. Comparing this with the results of the present study in which values of 62–71% conversion were obtained, it is clear that the seaweeds under study are of equal or better capability to bioreduce hexavalent chromium. It is also important to note that the Cr(VI) concentration used in this study was significantly higher (approximately 30 times) than that used by Yang and Chen [15]. This indicates the potential of these seaweeds to bring about significant detoxification of Cr(VI) at elevated metal levels.

As previously discussed, because both Cr(VI) and Cr(III) were present on the biomass surface this indicated that complete reduction had not occurred within the contact time of 6 h. Thus, significant quantities of hexavalent chromium are detoxified in a much shorter period with these three seaweeds warranting further investigation of these species as a means of chromium clean-up from contaminated wastewaters.

4. Conclusions

This study revealed that these three seaweeds effectively removed between 14 and 18% of the total chromium from a concentrated Cr(VI) solution indicating their suitability as biosorbents for detoxification of Cr(VI) over a short time period. Cr(III) was bound to these seaweeds by an ion-exchange mechanism thus altering surface morphology by altering the polymer structures of the seaweed surface. The mechanism of Cr(VI) binding was adsorption coupled with reduction to Cr(III). Conversion of Cr(VI) to Cr(III) ranged from 64 to 75% over a 6 h period with *Ulva* spp. showing the greatest bio-reduction capacity. Chromium binding affected the relative quantities of carboxyl and alcohol groups in biomass polysaccharides, the extent of which varied between species and thus pointed to their involvement in Cr(VI) binding to these seaweeds. Thus the potential of these seaweeds to reduce and detoxify elevated Cr(VI) concentrations over relatively short time periods has clearly been demonstrated. Biosorption technology provides an alternative for treatment of Cr(VI) with optimum removal occurring at lower pH values. However, organic leaching often occurs at low pH and it is thus important to develop biosorbents that work in this range without such operational issues. Further development may include chemical modification of biosorbents and immobilisation into packed columns.

Acknowledgements

The authors gratefully acknowledge the support of: The Irish Research Council for Science, Engineering and Technology under the Embark Initiative. Technology Sector Research Strand III – Estuarine Research Group (2003). European Regional Development Fund (ERDF) INTERREG IIIA Ireland/Wales Programme 2000–2006, under the SWINGS (Separations, Wales & Ireland – Novel Generation Science) project. Balazs Azalos (Materials & Surface Science Institute, University of Limerick). The Tyndall National Institute (Cork) under the National Access Programme.

References

[1] J. Barnhart, Reg. Tox. Pharm. 26 (1997) S3–S7.
[2] A. Baral, R.D. Engelken, Environ. Sci. Pol. 5 (2002) 121–133.
[3] G. Arslan, E. Pehlivan, Bioresour. Technol. 98 (2007) 2836–2845.
[4] S. Schiewer, M.H. Wong, Chemosphere 41 (2000) 271–282.
[5] T.A. Davis, B. Volesky, A. Mucci, Water Res. 37 (2003) 4311–4330.
[6] M.T.K. Tsui, K.C. Cheung, N.F.Y. Tam, M.H. Wong, Environ. Sci. Technol. 35 (2006) 4353–4358.
[7] R.W. Smith, C. Lacher, Miner. Eng. 15 (2002) 187–191.
[8] B. Volesky, G. Naja, Int. J. Tech. Transf. Commercialisation 6 (2007) 196–211.
[9] V. Murphy, H. Hughes, P. McLoughlin, Chemosphere 70 (2008) 1128–1134.
[10] L.S. Clesceri, A.E. Greenberg, A.D. Eaton, Standard Methods for the Examination of Water and Wastewater, 20th ed., Washington, DC, American Public Health Association, American Water Work Association and Water Environment Federation, 1998, pp. 366–368.
[11] V. Murphy, H. Hughes, P. Mc Loughlin, Water Res 41 (2007) 731–740.
[12] E.G.V. Percival, R.H. McDowell, Chemistry and Enzymology of Marine Algal Polysaccharides, Academic Press, London, UK, 1967.
[13] P.X. Sheng, Y.-P. Ting, J.P. Chen, L. Hong, J. Colloid Interface Sci. 275 (2004) 131–141.

[14] O. Raize, Y. Argaman, S. Yannai, Biotechnol. Bioeng. 87 (2004) 451–458.
[15] L. Yang, J.P. Chen, Bioresour. Technol. 99 (2008) 297–307.
[16] J.P. Chen, L.A. Hong, S.N. Wu, L. Wang, Langmuir 18 (2002) 9413–9421.
[17] M.M. Figueira, B. Volesky, H.J. Mathieu, Environ. Sci. Technol. 33 (1990) 1840–1846.
[18] D. Kuyucak, B. Volesky, Biotechnol. Bioeng. 33 (1989) 823–831.
[19] D. Park, Y.-S. Yun, J.M. Park, Ind. Eng. Chem. Res. 45 (2006) 2405–2407.
[20] C.M. Lytle, F.W. Lytle, N. Yang, J.-H. Qian, D. Hansen, A. Zayed, N. Terry, Environ. Sci. Technol. 32 (1998) 3087–3093.
[21] J.L. Gardea-Torresdey, K.J. Tiemann, V. Armendariz, L. Bess-Oberto, R.R. Chianelli, J. Rios, J.G. Parsons, G. Gamez, J. Hazard. Mater. 80 (2000) 175–188.
[22] K.H. Wong, C.K. Cheung, Food Chem. 71 (2000) 475–482.
[23] D. Briggs, Applications of XPS in polymer technology, in: D. Briggs, M.P. Seah (Eds.), Practical Surface Analysis, vol. 1, Auger and X-ray Photoelectron Spectroscopy, Wiley, Chichester, 1990, pp. 436–483.
[24] Surface characterization by spectroscopy and microscopy, in: D.A. Skoog, F.J. Holler, T.A. Nieman (Eds.), Principles of Instrumental Analysis, Saunders College Publishing, 1992, pp. 535–566.
[25] J.P. Chen, L. Yang, Langmuir 22 (2006) 8906–8914.
[26] L. Dambies, C. Guimon, S. Yiacoumi, E. Guibal, Colloids Surf. A 177 (2001) 203–214.
[27] D. Park, S.-R. Lim, Y.-S. Yun, J.M. Park, Chemosphere 70 (2007) 298–305.
[28] D. Park, Y.-S. Yun, J.M. Park, J. Colloid Interface Sci. 317 (2008) 54–61.
[29] D. Park, Y.-S. Yun, J.M. Park, Environ. Sci. Technol. 38 (2004) 4860–4864.
[30] D. Park, Y.-S. Yun, J.M. Park, Chemosphere 60 (2005) 1356–1364.